



Montréal, Québec
May 29 to June 1, 2013 / 29 mai au 1 juin 2013

Testing of Hybrid Reinforced Curb-Deck Connections of Post-and-Beam Bridge Barriers

Ehab Ahmed, Christian Dulude, Alexandre Fortier, and Brahim Benmokrane
Department of Civil Engineering, University of Sherbrooke, Sherbrooke, Quebec, Canada

Abstract: This paper evaluates the capacity of hybrid reinforced curb-deck connections of post-and-beam bridge barriers. The test prototypes consisted of a slab measured 2.5 × 3.0 m with a 225 mm thickness and a curb of 3.0 m long. Two barrier prototypes were fabricated and tested under quasi-static loading until failure. The first one was totally reinforced with epoxy-coated steel bars while the second one was reinforced with epoxy-coated steel bars in the slab and glass fiber-reinforced polymer (GFRP) bars in the curb. The main objectives are to verify whether: 1) the resistance to out-of-plane quasi-static loads and the associated transverse deflection of the hybrid reinforced curb-deck connection and steel barrier system are comparable to those of the steel RC counterpart; and 2) the transverse strength exceeds the CHBDC equivalent static load demand. The behavior of the barrier prototypes was evaluated in terms of cracking pattern, crack width, and strains in reinforcing bars. The results revealed that the behavior of the hybrid reinforced curb-deck connection is similar to that of the steel RC counterpart. In addition, the capacity of the hybrid reinforced curb-deck connection is higher than that of steel reinforced one by 37%.

1 Introduction

The use of glass fiber-reinforced polymer (GFRP) bars as internal reinforcement is a viable solution to provide corrosion resistance to concrete bridge decks (Nanni and Faza 2002), barriers (El-Salakawy et al. 2003, Matta and Nanni 2009), and piers (De Luca et al. 2010). The recent advances in the fiber-reinforced polymer (FRP) technology led to the development of FRP bars with enhanced mechanical and durability properties. As a result, bridge design specifications have been published in Canada (CSA 2006) and the US (AASHTO 2009) to enable practitioners to deploy the technology.

Due to the lower cost of GFRP bars compared to the other types (carbon and aramid), they gained significant attention in research and applications. Successful field implementation in bridges in North America (Benmokrane et al. 2004, 2006, 2007a; b) provided evidences on the durability of GFRP bars in real service conditions. Furthermore, CSA S807 (CSA 2010) provided a step forward towards standardizing the FRP bars which is expected to increase the use of GFRP bars in many applications.

Recently, with the increase in the use of GFRP bars in bridge applications, the hybrid reinforcement technique gained some attention. Ahmed and Benmokrane (2012) reported the use of hybrid reinforcement in bridge deck slabs in Quebec where the bridge decks were reinforced with a bottom mat of steel bars and a top mat of GFRP bars. The curbs of the steel-and-beam bridge barriers, however, were reinforced with steel bars.

This paper evaluates the performance of the steel-and-beam bridge barriers whose curbs are reinforced GFRP and epoxy-coated steel bars while the deck slab reinforcement is maintained as epoxy-coated

Each of the barrier prototypes was cast on two stages. Stage I included casting the horizontal slab after preparing the reinforcement cages for slab and curb. Before casting of the horizontal slabs, 75-mm diameter PVC tubes were installed in the slabs creating 75-mm diameter holes through the slab thickness (Figure 1) to enable anchoring the slabs to the laboratory strong floor during the test. The barrier prototypes were cast using a ready-mixed normal density concrete. The concrete compressive strengths, determined based on the testing of 150 × 300 mm cylinders, of the slabs and curbs were 45 and 33 MPa respectively. Figure 2 shows the fabrication of the barrier prototypes.



Figure 2: Fabrication of the barrier prototypes

1.2 Instrumentation

The barrier prototypes were instrumented with electrical-resistance strain gauges to measure strains in reinforcing bars and in concrete at critical locations as shown in Figure 3. Each barrier prototype was instrumented with 40 strain gauges attached to the reinforcing bars and 5 strain gauges attached to the concrete surface. The strain gauges attached to the reinforcing bars were arranged at three different transversal sections and the strain gauges in one of those sections are shown in Figure 3. However, the concrete strain gauges were attached in the critical locations to capture the compressive strains of the concrete during the test. The induced displacement and deflection in the tested barrier prototypes were also measured using many Linear Variable Differential Transducers (LVDTs) as shown in Figure 3.

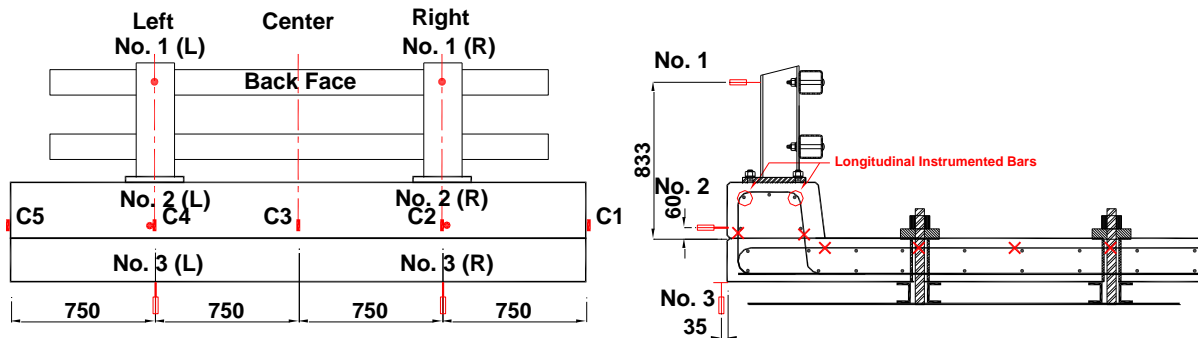


Figure 3: Instrumentation details

1.3 Test setup and procedure

The barrier prototypes were supported on two parallel steel beams spaced at 1.0 m with an overhang of 1.0 m to simulate the actual barriers in real bridge decks. The slab of the barrier prototypes was tightened to the laboratory rigid floor by six 38-mm diameter Dywidag bars (anchors) and nuts. A tensile force of 100 kN was applied on each anchor bar to assure that no rigid body displacement occurs during testing. 45-mm thick square steel plates (200 × 200 mm) were used as bearing plates between the nuts and the

slab. A clear distance of 114 mm was used between the bottom surface of the barrier and the laboratory strong floor to allow for deflection and rotation of the barrier wall and slab during testing. Figure 4 shows the test setup.

The load was applied horizontally to the center of the steel railing at a distance of 810 mm from the slab surface as shown in Figure 4. The load was transmitted from the hydraulic jack to the barrier prototypes through a 1.5 m-long spreader I-beam. The load was applied using a 1000 kN-capacity hydraulic actuator connected to a manual pump with a load-controlled rate of 5 kN/min. The load was measured with a load cell having a capacity of 500 kN.

It should be mentioned that the designed setup is similar to that of Ahmed and Benmokrane (2011) at the University of Sherbrooke which is in agreement with that of Deitz et al. (2004), Matta and Nanni (2009), and Mitchell et al. (2010). These setups are devoted to simulate the actual deck-barrier connection which is usually provided through a cantilever deck slab supporting the barrier. Besides, this setup allows investigating the behaviour of the deck-barrier connection under the real case of stresses which includes flexure, shear, and axial forces. More details about the instrumentation and test setup can be found elsewhere (Ahmed et al. 2010)

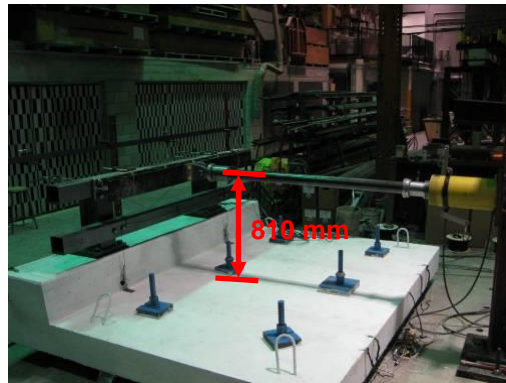


Figure 4: Test Setup

2 Test Results and Discussion

2.1 Ultimate capacity and mode of failure

Table 1 presents the ultimate capacities and modes of failure of the two S-1642 barrier prototypes. The GFRP-reinforced prototype had an ultimate capacity of 313.6 kN which is higher than that of the steel-reinforced prototype (228.3 kN). The ratio between the ultimate capacity of the S-1642-GFRP and that of the S-1642-Steel was 1.37. Thus, regardless the mode of failure, replacing the epoxy-coated steel reinforcement of the S-1642-Steel prototype with the GFRP reinforcement enabled achieving an increase in the ultimate capacity of about 37%. Furthermore, the capacities of both prototypes (S-1642-Steel and S-1642-GFRP) were more than two times the mandated value $P_t = 100$ kN for PL-2 barriers (CSA 2006).

Figure 5 shows the failure of the S-1642-Steel and S-1642-GFRP prototypes, respectively. The S-1642-Steel prototype failed by diagonal tension failure at corner of curb-deck joint after yielding of the slab reinforcement. On the other hand, S-1642-GFRP prototype failed due to the buckling of the steel posts. Corresponding to the load at which buckling of the steel posts occurred, which was the failure load, the strains of the steel of the slab were beyond the yield strain and the final crack pattern was similar to that of the steel-reinforced one (S-1642-Steel). In addition, diagonal tension crack at corner of curb-deck joint was observed but it did not control the failure.

Considering the ultimate capacities listed in Table 1 and the mode of failure shown in Figure 5, it can be noticed that the behaviour of the S-1642-GFRP prototype was very similar to that of the S-1642-Steel

prototype up to the failure. However, the capacity of the S-1642-GFRP was higher than that of S-1642-Steel because the steel posts could not resist and failed due to excessive buckling.

Table 1: Details of the test prototypes

Barrier prototype	Ultimate capacity (kN)	Mode of failure
S-1642-Steel	228.3	Diagonal tension failure at corner of curb-deck joint (Fig. 5a).
S-1642-GFRP	313.6	Buckling failure of steel post. Diagonal tension crack at corner of curb-deck joint was observed (Fig. 5b).



(a) S-1642-Steel



(b) S-1642-GFRP

Figure 5: Cracking pattern at failure

2.2 Deflection

Figures 6 and 7 show the load-deflection relationships of the curb and the slab, respectively. The maximum deflection was recorded by the two LVDTs at the top of the bridge railing (No. 1). Besides, there was no significant difference between the deflection of the curb and the slab measured from the left and the right side of the barrier prototypes. The comparisons presented in Figure 6 and 7 show that both of the GFRP-reinforced and steel-reinforced prototypes had the same load deflection relationships till the failure of the steel-reinforced one which was lower than that of the GFRP-reinforced one.

At the peak load of the S-1642-Steel prototype (228.3 kN) the deflection of the curb and the slab were 37 and 16 mm, respectively. The deflection of the curb and the slab of the S-1642-GFRP corresponding to that load were 28 and 15 mm, respectively. At the peak load of the S-1642-GFRP prototype (313.6 kN) the deflection of the curb and the slab were 65 and 24 mm, respectively. The post-peak deflection of the curb and the slab of the S-1642-Steel reached about 160 and 50 mm at failure, respectively. The buckling failure of the steel posts of the S-1642-GFRP prototype did not enable achieving the deformation capacity of the barrier. Consequently, the post-peak deformation (deflection) was low.

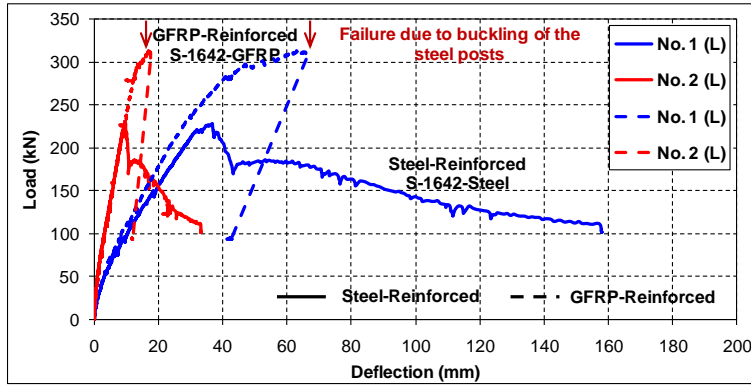


Figure 6: Load-deflection relationships of posts and curbs

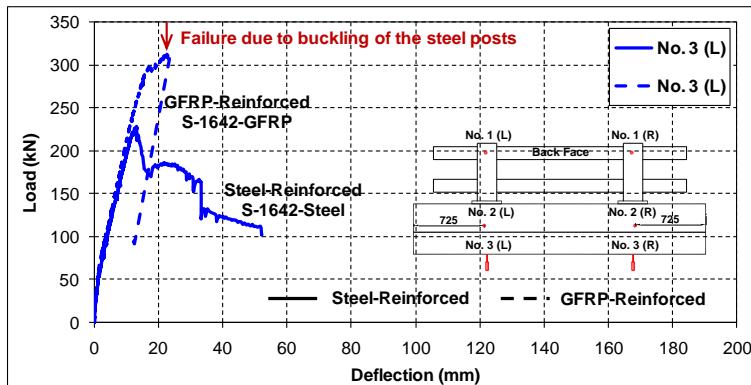


Figure 7: Load-slab deflection relationships

2.3 Strains in concrete

Figure 8 shows a comparison between the maximum measured concrete strains. The figure indicates that at the same load level, the GFRP-reinforced barrier prototype showed lower strains values than that reinforced with epoxy-coated steel. At failure, the maximum measured concrete strains were about 325 microstrains in the steel-reinforced barrier prototype (S-1642-Steel) and was 370 microstrains in the GFRP-reinforced barrier prototype (S-1642-GFRP).

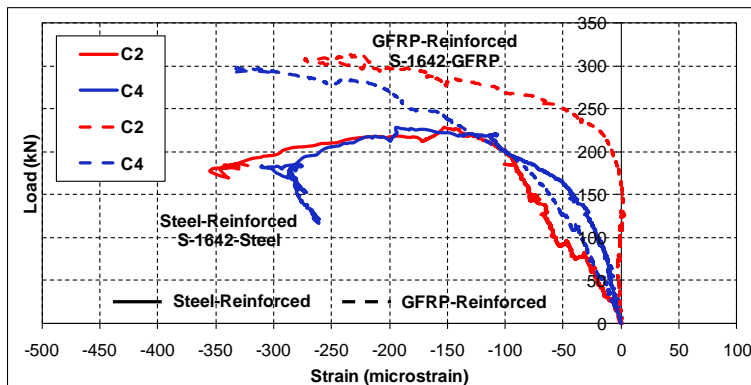


Figure 8: Maximum measured concrete strains

2.4 Strains in the reinforcing bars

2.4.1 Transverse reinforcement of the slabs

Figure 9 shows the load-strain relationships in the slab's top transverse reinforcement. It is worth mentioning that the maximum measured strains in the top transverse reinforcement of S-1642-Steel prototype occurred at the sections that pass through the posts (left and right sections). In the S-1642-GFRP prototype, however, the slab reinforcement of the three instrumented sections reached the yield strain. This implies that the load distribution in case of the GFRP stirrups in the curb is better than the case of epoxy-coated stirrups. The comparison shown in Figure 9 confirms that the strains in the transverse steel bars of the slabs of S-1642-Steel and S-1642-GFRP are the same.

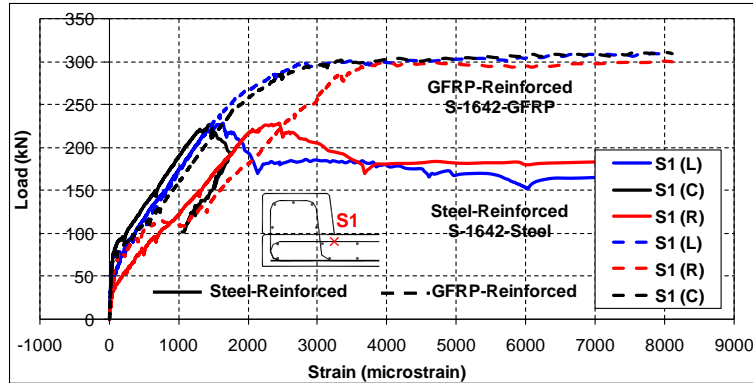


Figure 9: Measured strains in the top reinforcement of the slab

2.4.2 Transverse reinforcement of the curb (stirrups)

Figure 10 provides a comparison between the maximum measured strains in transverse reinforcement of the curbs (stirrups). It can be noticed that the stains in the GFRP stirrups of the S-1642-GFRP prototype were in good agreement with that of the S-1642-Steel prototype till the failure of the S-1642-Steel one. Besides, the strain increasing rate at very late loading stage becomes high due to the widening of the separation crack between the slab and the curb. This was observed for the two tested prototypes (GFRP- and steel-reinforced).

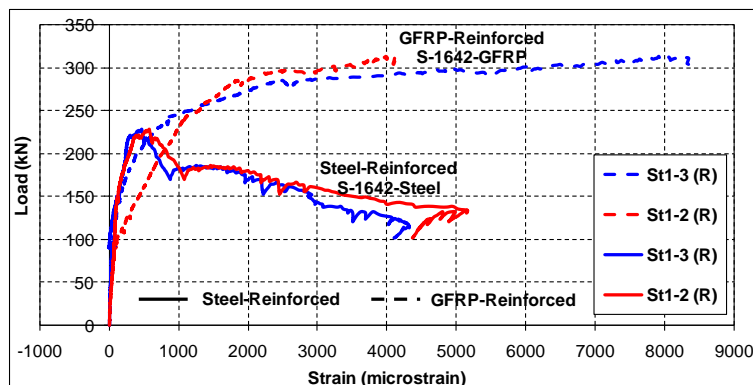


Figure 10: Reinforcement strains in the curb

3 Summary and Conclusions

This paper presents the test results deck-curb connection of post-and-beam bridge barriers whose curbs are reinforced with GFRP and steel bars. Based on the results and the discussion presented above, the following conclusions are drawn:

1. The S-1642-GFRP prototype showed an ultimate capacity of 313.6 kN which exceeds the strength of the steel reinforced ones (S-1642-Steel) with 37%, regardless the mode of failure.
2. The S-1642-Steel prototype failed by the concrete splitting of the slab. However, The S-1642-GFRP prototype failed due to the buckling of the steel posts at higher applied load than that of the S-1642-Steel (37% higher).
3. The capacities of both prototypes (S-1642-Steel and S-1642-GFRP) are higher than the mandated values provided by the CHBDC (CSA 2006).
4. The S-1642-GFRP barrier prototype had almost the same load-deflection relationships and load-transverse reinforcement strain relationships as S-1642-Steel prototype till the failure load of the S-1642-Steel, which was lower than that of the GFRP-reinforced prototype (S-1642-GFRP).
5. The sudden failure of the S-1642-GFRP due to the buckling of the steel posts did not enable achieving the deformation capacity of the S-1642-GFRP prototype. The post-peak deflections recorded at all points of the prototype were lower than that of the S-1642-Steel due to this mode of failure.
6. The GFRP stirrups of the S-1642-GFRP prototype had a strain values very close to that resulted from the epoxy-coated steel stirrups of the S-1642-Steel prototype regardless the lower axial stiffness of the GFRP bars compared to that of steel.
7. From the test results, both prototypes (S-1642-GFRP and S-1642-Steel) have very similar behaviour, however, the GFRP-reinforced prototype failed at higher ultimate capacity than that of the steel-reinforced one by buckling of the steel posts.

4 Acknowledgements

The authors acknowledge the financial support received from Alberta Transportation. The authors also acknowledge BP Composites Ltd. (Alberta, Canada), GFRP bar supplier; Beton Demix, the concrete provider; and Les Coffrages Carmel Inc., fabricator of formworks, concrete casting and curing. The authors would like to thank the technical staff in the structural laboratory at the University of Sherbrooke especially Mr. Francois Ntacorigira and Simon Kelly for their assistance in the instrumentation and testing of the barrier prototypes.

5 References

- Ahmed, E., and Benmokrane, B. 2012. Hybrid Reinforced Concrete Bridge Deck Slab of 410 Overpass Bridge in Quebec: Construction and Testing. *Proceedings of the 3rd International Structural Specialty Conference*, CSCE, Edmonton, Alberta, June 6–9, 10 p.
- Ahmed, E., Dulude, C., and Benmokrane, B. 2010. Static Testing of Alberta Transportation Concrete Bridge Barrier Walls of Type PL-2 Reinforced with GFRP and Steel Bars. Technical Report, submitted to Alberta Transportation, Technical Standards Branch, Edmonton, Alberta, Canada, 114 p.
- Ahmed, E.A. and Benmokrane, B. 2011. Static Testing of Full-Scale Concrete Bridge Barriers Reinforced with GFRP Bars. ACI SP-275, American Concrete Institute, pp. 5.1–5.20.
- American Association of State Highway and Transportation Officials (AASHTO). (2009). *AASHTO LRFD Bridge Design Guide Specifications for GFRP-Reinforced Concrete Bridge Decks and Traffic Railings*, 1st Ed., AASHTO, Washington, D.C.
- Benmokrane, B., El-Salakawy, E., Desgagné, G., and Lackey, T. 2004. FRP Bars for Bridges. *Concrete International*, American Concrete Institute, 26(8): 84–90.
- Benmokrane, B., El-Salakawy, E., El-Gamal, S., and Goulet, S. 2007a. Construction and Testing of Canada's First Concrete Bridge Deck Totally Reinforced with Glass FRP Bars: Val-Alain Bridge on

- Highway 20 East. *ASCE Journal of Bridge Engineering*, 12(5):632–645.
- Benmokrane, B., El-Salakawy, E., El-Ragaby, A., and El-Gamal, S. 2007b. Performance Evaluation of Innovative Concrete Bridge Deck Slabs Reinforced with Fibre-Reinforced Polymer Bars. *Canadian Journal of Civil Engineering*, 34(3): 298–310.
- Benmokrane, B., El-Salakawy, E., El-Ragaby, A., and Lackey, T. 2006. Designing and Testing of Concrete Bridge Decks Reinforced with Glass FRP Bars. *ASCE Journal of Bridge Engineering*, 11(2): 217-229.
- Canadian Standard Association (CSA). 2006. Canadian Highway Bridge Design Code. CAN/CSA S6-06, Rexdale, Ontario, Canada, 788.
- De Luca, A., Matta, F., and Nanni, A. 2010. Behavior of Full-Scale GFRP Reinforced Concrete Columns under Axial Load. *ACI Structural Journal*, 107(5): 589-596.
- Deitz, D. H., Harik, I. E., Gesund, H., and Zatar, W. A. 2004. Barrier Wall Impact Simulation of Reinforced Concrete Decks with Steel and Glass Fiber Reinforced Polymer Bars. *ASCE Journal of Composites for Construction*, Technical Note, 8(4): 369-373.
- El-Salakawy, E., Benmokrane, B., Masmoudi, R., Brière, F., and Éric Breaumier, E. 2003. Concrete Bridge Barriers Reinforced with Glass Fiber-Reinforced Polymer Composite Bars. *ACI Structural Journal*, 100(6): 815–824.
- Matta, F. and Nanni, A. 2009. Connection of Concrete Railing Post and Bridge Deck with Internal FRP Reinforcement. *ASCE Journal of Bridge Engineering*, 14(1): 66–76.
- Mitchell, G., Strahota, M.T., Gokani, V., Picón, R., Yang, S., Klingner, R. E., and Williamson, E. B. 2010. Performance of Retrofit Highway Barriers with Mechanical Anchors. *ACI Structural Journal*, 107(4): 381–389.
- Mitchell, G., Strahota, M.T., Gokani, V., Picón, R., Yang, S., Klingner, R. E., and Williamson, E. B. 2010. Performance of Retrofit Highway Barriers with Mechanical Anchors. *ACI Structural Journal*, 107(4): 381–389.
- Nanni, A., and Faza, S. 2002. Designing and constructing with FRP bars: An emerging technology. *Concrete International*, American Concrete Institute, 24(11), 53–58.